Neonatal neurosonography: A pictorial essay

Venkatraman Bhat, Varun Bhat
Departments of Radiology and Imaging Services, Narayana Health, Bangalore, Karnataka, India

Correspondence: Dr. Venkatraman Bhat, 309, Greenwoods Apt, Royal Gardenia, Bommasandra, Bangalore - 560 099, Karnataka, India.
E-mail: bvenkatraman@gmail.com

Abstract

Neurosonography is a simple, established non-invasive technique for the intracranial assessment of preterm neonate. Apart from established indication in the evaluation of periventricular haemorrhage, it provides clue to wide range of pathology. This presentation provides a quick roadmap to the technique, imaging anatomy and spectrum of pathological imaging appearances encountered in neonates.

Key words: Cranial USG; germinal matrix haemorrhage; neurosonography

Introduction

Sonographic examination of the neonatal brain remains an invaluable assessment tool in experienced hands. Many radiologists are not quite familiar with the spectrum of imaging appearances of the neonatal intracranium due to inadequate exposure. Many specific clinical questions can be resolved by optimally utilizing this simple informative tool. Portability of the study, lack of need to transport baby to radiology services, and the wealth of diagnostic information available from a large open anterior fontanelle makes this study a highly challenging one.[1] This pictorial essay attempts to highlight the common indications for neurosonography, its basic techniques, sonographic anatomy, and the spectrum of pathological imaging appearances seen in neonates. With an ever-growing innovation in technique and an increasing affordability of state-of-the-art equipment, there is a greater need for the radiological community to be well acquainted with various facets of this diagnostic tool.

Access this article online	
Quick Response Code:	Website: www.ijri.org
	DOI: 10.4103/0971-3026.143901

Indications

The main indication for this examination is the demonstration or exclusion of an intracranial hemorrhage in a preterm neonate. The technique is additionally used for the follow-up of intraventricular hemorrhage (IVH)-related complications to look for evolving findings pertaining to ischemia. Other broader indications include demonstration of congenital structural anomalies, intracranial vascular lesions, and also its use as a simple screening tool in the exclusion of gross intracranial pathology.

Cranial USG Technique

There are essential steps to be followed before the procedure. Most of the examination is performed bedside with the neonate within the incubator. Examination is preferably done through the cranial incubator opening. Care should be taken not to move the infant or to cause any disturbance to incubator temperature. Pressure over the anterior fontanelle is to be avoided, especially in a critically ill premature neonate. All aseptic precautions are to be followed in accordance with the protocols of the neonatal ICU.

Best results are obtained with a high-frequency phased array transducer (5-8 MHz) with a small footprint probe. High-resolution images are obtained in preterm neonates by using probe frequency of 7.5 MHz. Technical difficulty may be encountered in obtaining the best image in the case

of a small anterior fontanelle [Figures 1 and 2]. Phased array transducers of small footprint and wide insonation angle (up to 140°) help to obtain examination of diagnostic quality.

Neurosonography starts with gray-scale imaging performed via the anterior fontanelle in the coronal and sagittal planes.[2-4] Generally, six to eight coronal images are obtained, beginning at the anterior frontal lobes and extending to the occipital lobes posterior to the lateral ventricle trigones[5] [Figure 3]. The transducer is then rotated 90° and five sagittal images are obtained, including a midline and two parasagittal views of right and left hemispheres encompassing the peripheral cortex[4,5] [Figure 4]. Color Doppler images for arterial and venous structures may be obtained for the screening of vascular structures.[6] Documentation of Doppler imaging of the circle of Willis and the region of vein of Galen is an essential part of the assessment [Figure 5]. Spectral tracing with peak systolic velocity (PSV), end-diastolic velocity (EDV), and resistive index (RI) need to be recorded for evaluation of ischemia. Power Doppler imaging has also been recommended by some authors to search for areas of hyper- or hypo-vascularity in suspected vascular occlusion, ischemia, or infarction.[3]

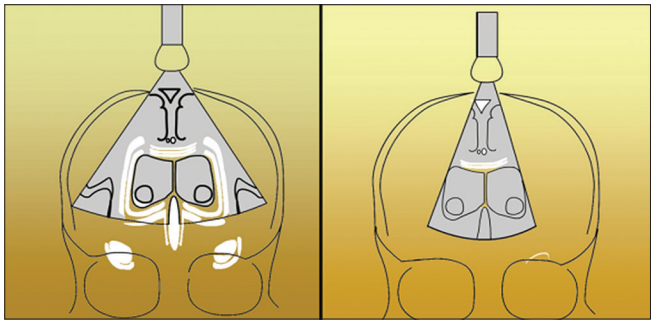

Figure 1: Diagrammatic illustration showing the size of fontanellae limiting the sonographic window

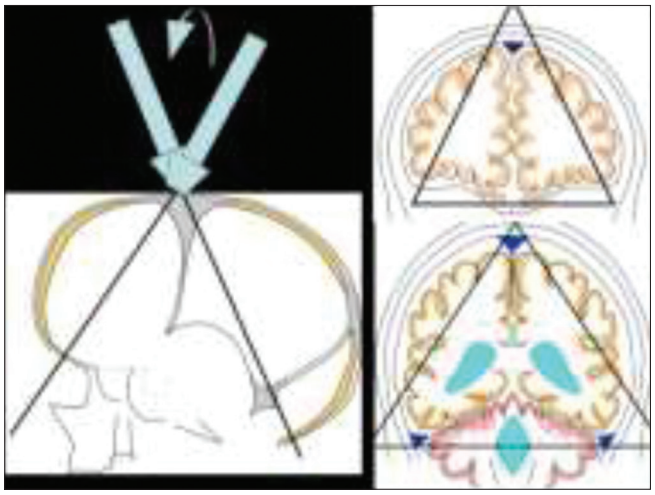

Figure 3: Illustration of coronal USG examination, showing frontal and posterior parietal planes

Screening via other supplemental fontanelle and obtaining high-resolution images from them may have added value. This technique has been shown to improve detection of posterior fossa hemorrhages and in the evaluation of the transverse sinuses.[7] Mastoid and posterior fontanelle approaches are useful in the demonstration of a subtle intraventricular bleed in the occipital horn, in patients with suspected holoprosencephaly and demonstration of a minor bleed in the brain stem and adjacent cerebellum.[7] To complete the examination, high-resolution linear-array transducer images are obtained for detailed interrogation of the convexity subarachnoid space and superficial cortex as well as deeper brain structures.[3] Linear images can be adjunctively obtained via any fontanelle for the evaluation of underlying anatomical structure or vessels.

Translation of brain anatomy to sonography needs understanding of sonographic physical principles. The general principles of sonography apply to intracranial study. Cerebrospinal fluid (CSF) spaces are anechoic, whereas the choroid plexus, small hemorrhages, and areas of infarction appear hyperechoic. On ultrasonography (USG), gray matter tends to be hypoechoic and white matter tends to be hyperechoic Secondly, the normal brain is always nearly symmetric. This fact allows for detection

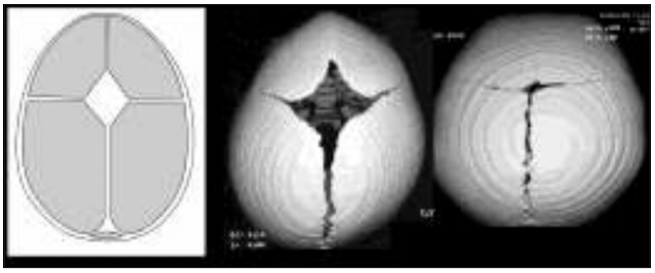

Figure 2: Anatomical picture of the anterior fontenellae; size variation in normal neonates as shown by CT volume-rendered reconstruction

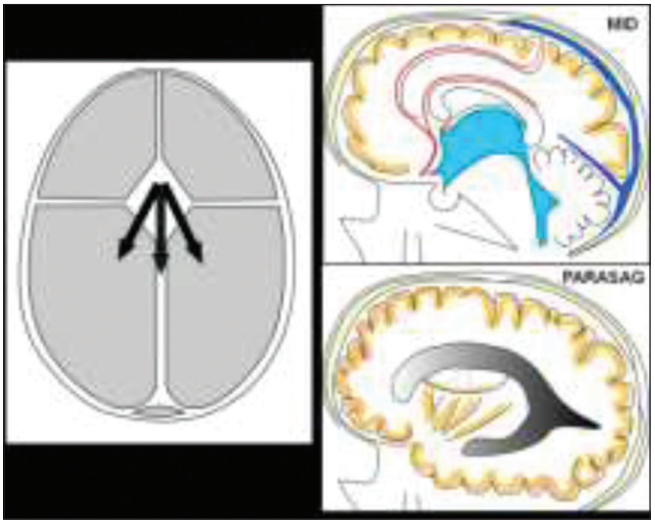

Figure 4: Illustration of sagittal and parasagittal USG examination, showing mid-sagittal and ventricular planes

of early changes of infarction or focal ischemia. Bilateral symmetric changes due to a systemic process may lead to errors in interpretation. A third fact involves interpretation of visible layers of the normal cortex. The superficial pia mater should be seen as a thin, well-defined hyperechoic layer immediately overlying the hypoechoic cortical gray matter, which in turn overlies the hyperechoic white matter.[8].

Failure to distinctly visualize these normal layers is indicative of abnormalities such as focal hemorrhage or infarct.[9] Lastly, the periventricular white matter is normally homogeneous in echogenicity and is equally or less echogenic than the adjacent choroid plexus.[4,6] Asymmetry or heterogeneity of the periventricular white matter is suggestive of an abnormality, such as periventricular leukomalacia (PVL). Normal anatomical illustrations are shown in Figures 6-9.

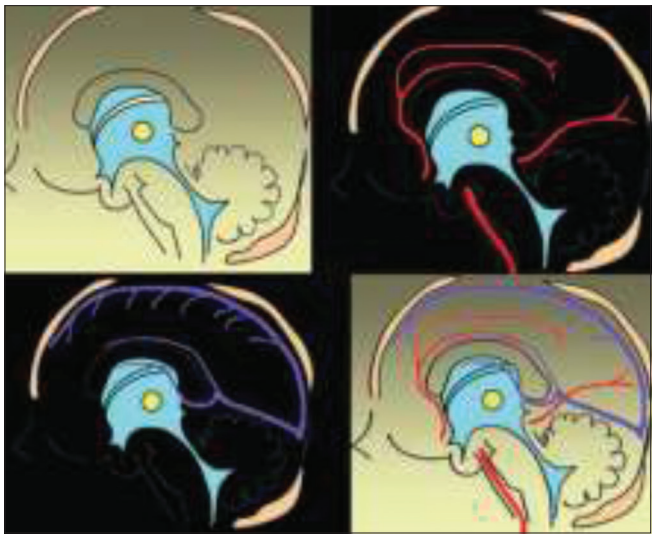

Figure 5: Illustration demonstrating arterial and venous anatomy in mid sagittal plane

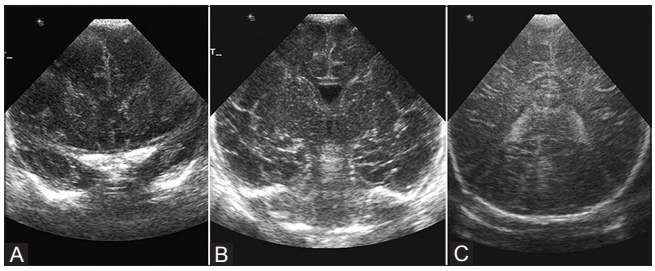

Figure 6 (A-C): Coronal USG at the level of frontal lobes (A), foramina of Monro (B), and trigone (C), demonstrating the interhemispheric fissure, lateral ventricles, and periventricular parenchyma

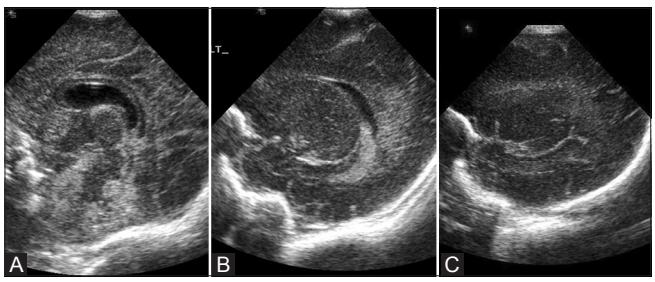

Figure 7 (A-C): Sagittal USG demonstrating corpus callosum, third and fourth ventricles, cerebellar vermis in midline (A). Cerebellum is relatively echogenic due to cerebellar foliae. Parasagittal images at the level of ventricle (B) and Sylvian region (C)

An understanding of normal variation is essential to neurosonographic interpretation. Cavum septum pellucidum is present in up to 50–61% of normal neonates[10] [Figure 10]. Minor asymmetry in the frontal horns or bodies of ventricles is often observed. Also, the echogenicity of periventricular parenchyma is variable. Being relatively echogenic in premature neonates, it might be wrongly interpreted as PVL. Massa intermedia can be quite variable in size in normal and pathological conditions [Figure 11]. When posterior fontanelle approaches are utilized, prominent calcar avis and lobulated glomus of the choroid should be observed as normal variations.[7]

Intracranial Hemorrhage

Germinal matrix hemorrhage

One of the most important indications of neurosonography is the demonstration of intracranial hemorrhage in a premature infant. Routine screening cranial USG should be performed in all infants of under 30 weeks gestation, once between 7 and 14 days of age and should be optimally repeated between 36 and 40 weeks postmenstrual age.[11-13] In term infants, non-contrast computed tomography (CT)

Table 1: Grading of cranial USG findings for the preterm infant

Classification of findings	
Intraventricular hemorrhage*	
Grade 1	Germinal matrix hemorrhage
Grade 2	Blood within the ventricular system, but not distending it
Grade 3	Intraventricular hemorrhage with ventricular dilatation
Grade 4	Parenchymal involvement
Preterm white matter injury†	
Grade 1	Increased periventricular echogenicity (lasting up to 7 days)
Grade 2	Increased periventricular echogenicity (lasting beyond 7 days)
Grade 3	Increased echogenicity with a tiny cyst formation
Grade 4	Coalescing larger cystic areas
Grade 5	Coalescing larger cystic areas extending to subcortical brain
Ventriculomegaly‡	
Mild	0.5-1.0 cm§
Moderate	1.0-1.5 cm§
Severe	1.5 cm§

*Reference 14,15, †References 16,17, ‡References 12.13, §Measurements at the midbody of the lateral ventricle on sagittal image (Modified from Ment *et al*.[11]), USG: Ultrasonography

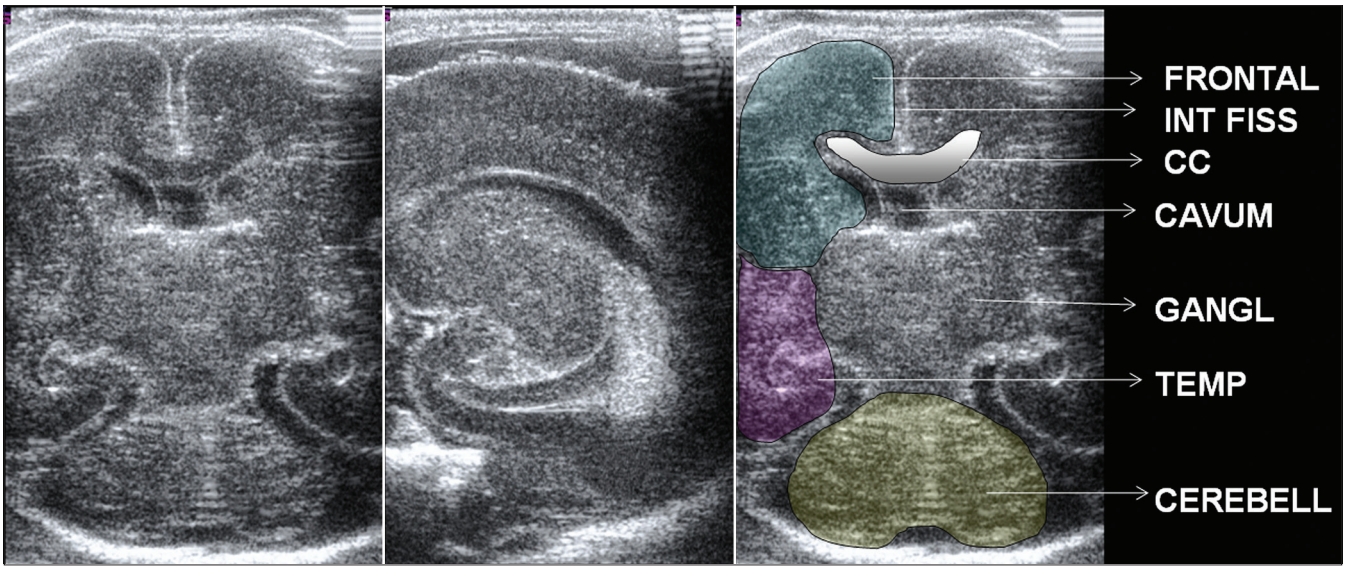

Figure 8: Coronal and parasagittal images of preterm (28 weeks) infant showing intracranial anatomy. Note the smooth surface of the immature brain. Distribution of the lobes colored

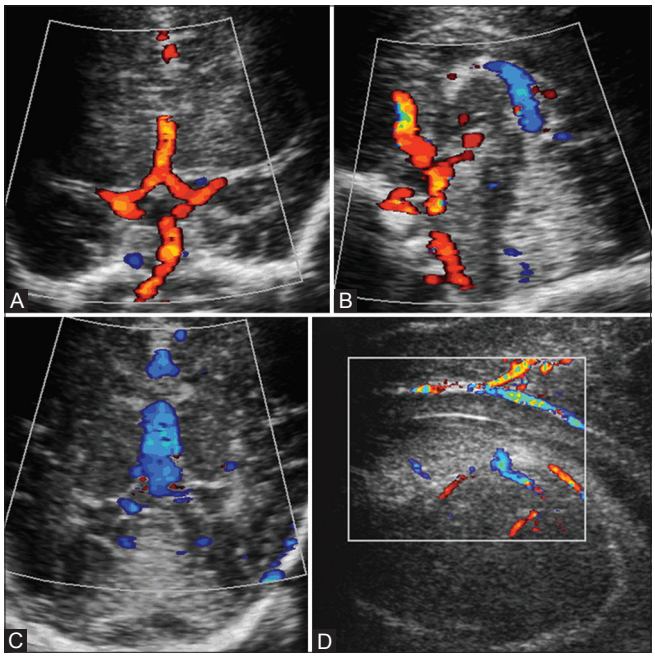

Figure 9 (A-D): Doppler images (A and B) demonstrating circle of Willis. Coronal USG demonstrating the vein of Galen. (C) Parasagittal study showing the small periventricular veins in the region of caudothalamic groove (D)

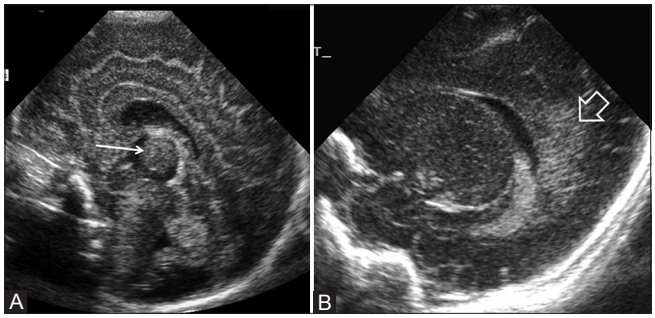

Figure 11 (A, B): (A) Sagittal USG demonstrating a relatively large massa intermedia (arrow) (B) Illustrates the relatively hyperechoic peritrigonal white matter(open arrow) in a normal neonate

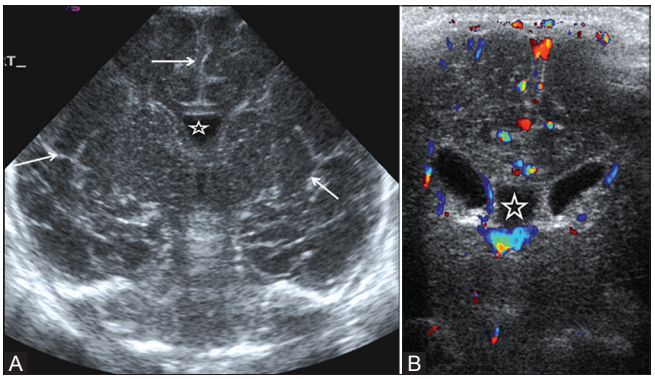

Figure 10 (A, B): Coronal USG demonstrating cavum septum (star) (A) and relation of vascular structures (B). Note that there are low-level echoes of cerebral gray and white matter, with subtle differences in the echoes of cortex and white matter. CSF spaces in Sylvian and inter-hemispherical region (arrows) are hyperechoic. Cerebellum is hyperechoic in relation to cerebral hemispheres

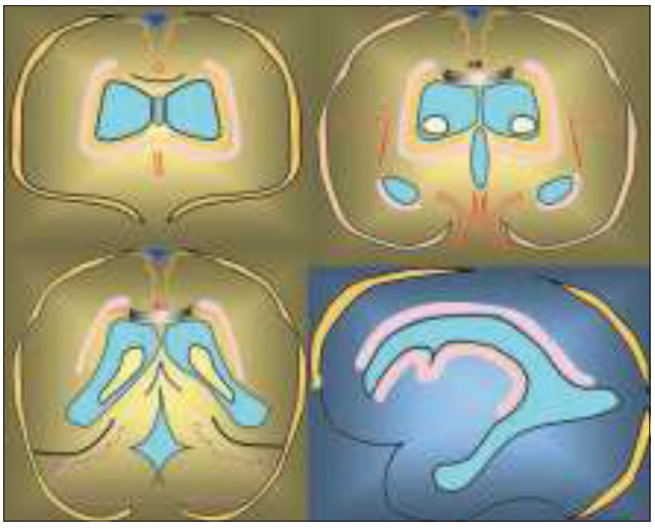

Figure 12A: The figure demonstrates the location and the extent of the germinal matrix (colored pink)

is preferred. Areas of potential bleeding arise in the zones of primitive germinal matrices, which are more extensive around the periventricular regions of the lateral ventricles and around the temporal horns [Figure 12A]. The extent of germinal matrix diminishes with progressive maturity, limiting it to the region of caudothalamic groove. Germinal matrix hemorrhages are seen as areas of increased echogenicity in the region of the caudothalamic groove. Germinal matrix hemorrhages were classified into four categories by Papile based on the extent of hemorrhage [Figure 12B][14] [Table 1].

Grade 1 hemorrhage is limited to the region of the caudothalamic groove, usually less than a centimeter in size [Figure 13]. Grade 2 hemorrhages extend into the adjacent ventricles, but do not cause ventricular dilatation. Grade 3 hemorrhages show ventricular extension and show minimal increase in the ventricular dimensions [Figures 14 and 15]. Grade 4 hemorrhages, presently considered as venous infarct, present with a predominant intraparenchymal component of hemorrhage, often with a sizable mass effect [Figures 16-19]. Posterior fossa hemorrhage is uncommon and can be demonstrated when sizable. Hemorrhages of grade 3 and 4 are associated with neurological deficits or learning disability.[1] Evolution of hemorrhage is demonstrated with follow-up sonograms [Figure 20].

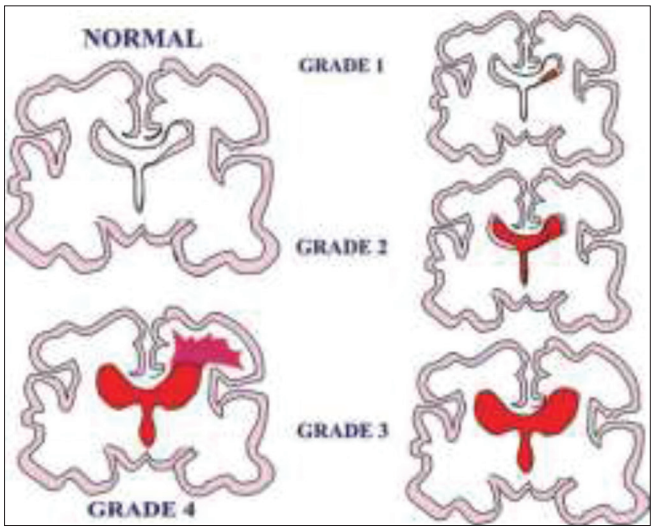

Figure 12B: Diagrammatic representation of IVH classification by Papile (modified)

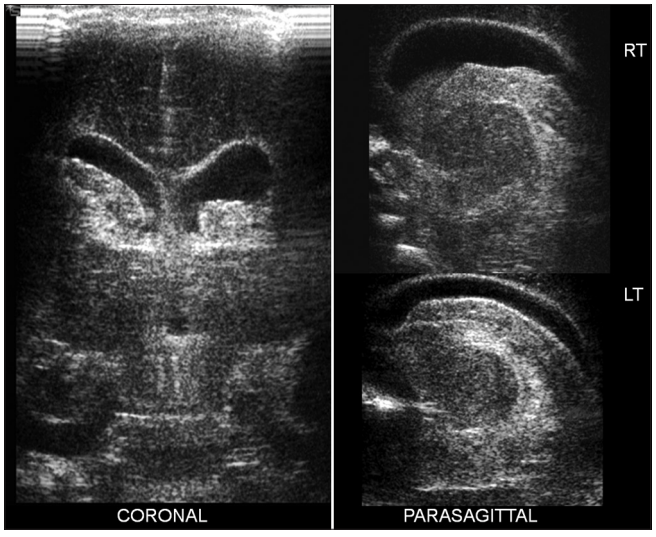

Figure 14: Coronal and both parasagittal images demonstrating the bilateral grade 3 hemorrhages with associated ventricular enlargement

Periventricular Leukomalacia

While the germinal matrix hemorrhages are a result of relatively acute hemodynamic changes, PVL represents a relatively insidious cerebral parenchymal insult. Chronic hypoxemia or hypoperfusion leads to PVL. On

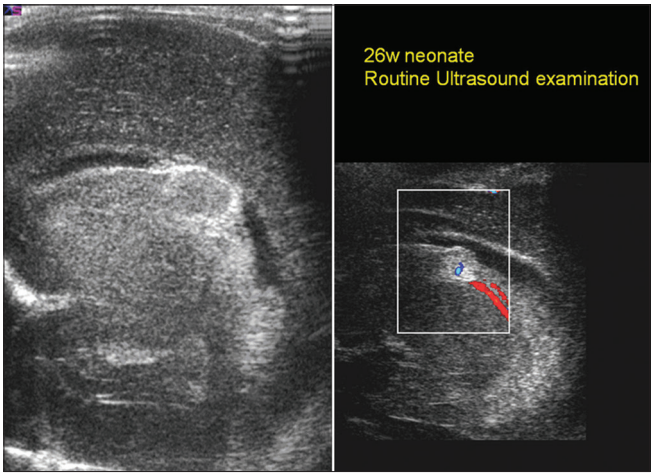

Figure 13: Coronal and sagittal sonographic images demonstrating a grade 1 hemorrhage at the caudothalamic groove

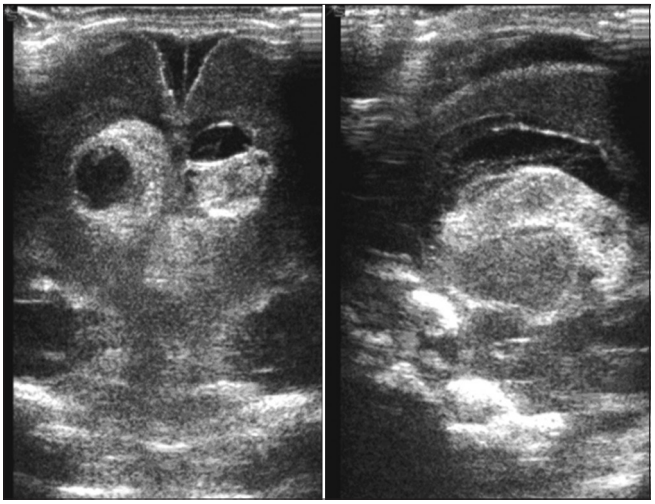

Figure 15: Coronal and parasagittal images demonstrating bilateral grade 3 interventricular hemorrhage. Note the relatively hypoechoic areas around the hyperechoic clot, which indicates fresh, extensive bleed

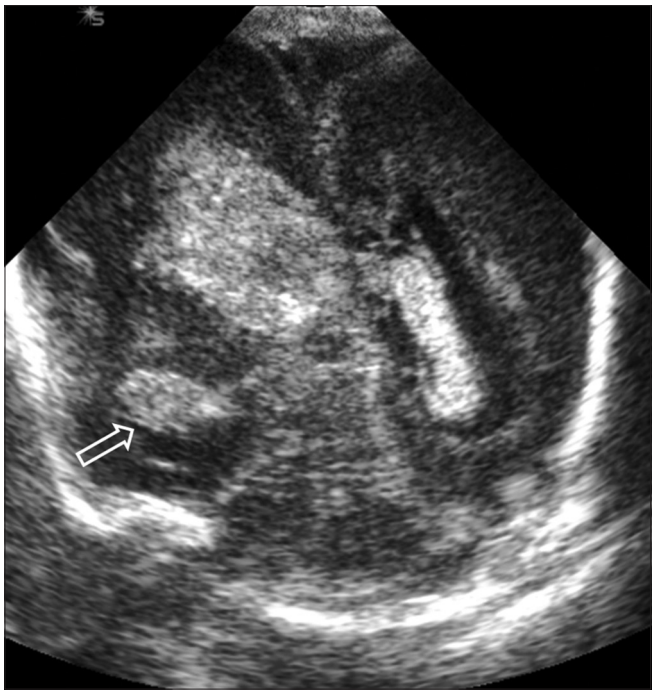

Figure 16: Coronal examination demonstrating grade 4 right interventricular hemorrhage with extension to the adjacent parietal lobe. Note the right temporal horn showing blood products (open arrow)

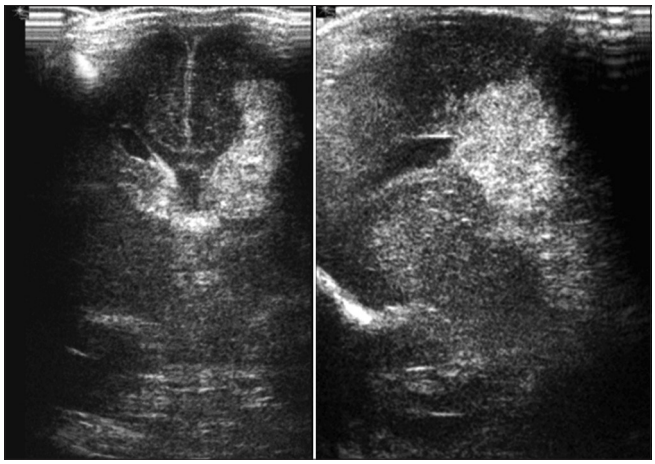

Figure 18: USG images demonstrating a grade 4 left intracranial hemorrhage. Note extensive ill-defined intraparenchymal component with relatively less mass effect, indicating hemorrhagic venous infarct

pathological studies on infants more than 6 days of age, there is high incidence of PVL in low-birth-weight infants between 900 and 2200 g.[1] Sonographic grading of PVL was described by Di Vries.[15-16] Grade 1 PVL generally presents as an increase in the parenchymal echoes in the periventricular region, mainly around the trigone, lasting less than 7 days [Figure 21]. These early sonographic findings are described as a periventricular flare. Some element of uncertainty of interpretation is noted in the extremely premature infant, in whom periventricular parenchyma is often echogenic [Figure 13]. Grade 2 PVL presents as persistent periventricular hyperechogenicity

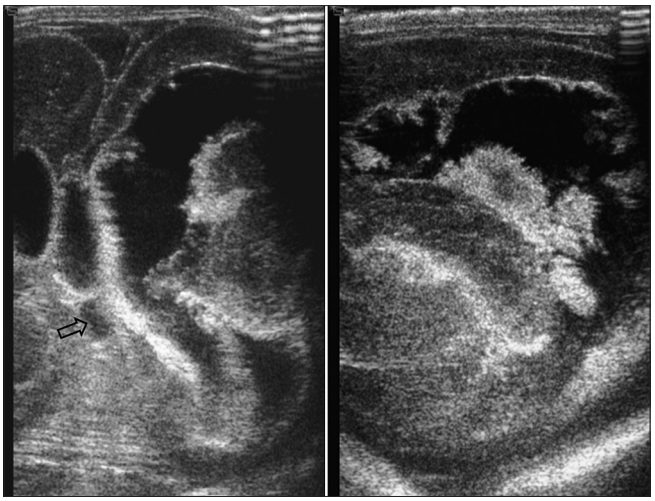

Figure 17: Coronal and parasagittal images showing the extensive grade 4 hemorrhage with a large fresh hematoma in the periventricular parenchyma. Note the hemispherical mass effect and third ventricular deviation (open arrow)

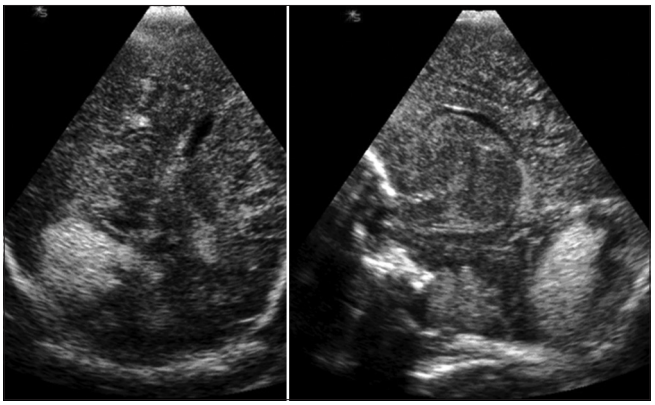

Figure 19: Large right tempo-occipital and cerebellar hemorrhage, shown as the hyperechoic area in the coronal and parasagittal images

lasting more than 7 days. Grade 3 PVL presents with relatively advanced parenchymal changes leading to microcyst formation [Figure 22A and B]. These changes are more evident in the parietal region and also extend to the frontal areas. Grade 4 PVL represents with multiple coalescing cystic areas in the cerebral parenchyma. Grade 4 changes represent advanced cystic changes reaching up to the level of cortex. Grade 3 and 4 changes are often associated with neurological sequelae such as diplegia and paraplegia in later life in upto 50% of patients [Figure 23]. Owing to the low sensitivity of sonography in the detection of non-hemorrhagic, non-cavitary parenchymal injury, additional imaging studies are usually necessary.[1]

Acute Ischemia

Evaluation of diffuse brain edema is technically challenging on neurosonography. As the size of the ventricles varies considerably, ventricular size is unreliable as a parameter

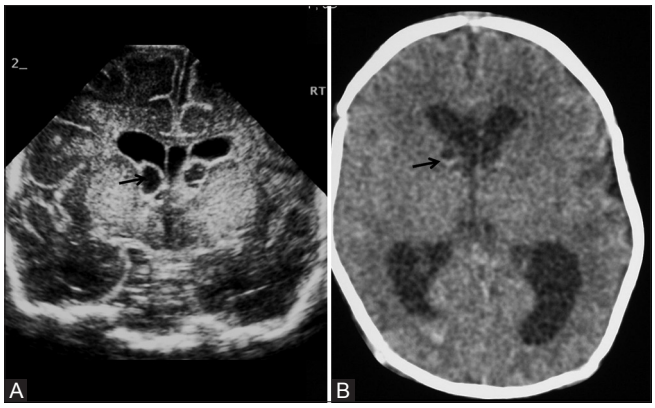

Figure 20 (A, B): Coronal USG demonstrating periventricular cystic changes (black arrow), sequelae of germinal matrix hemorrhage (A). Corresponding CT image shows tiny periventricular cystic lesions (B)

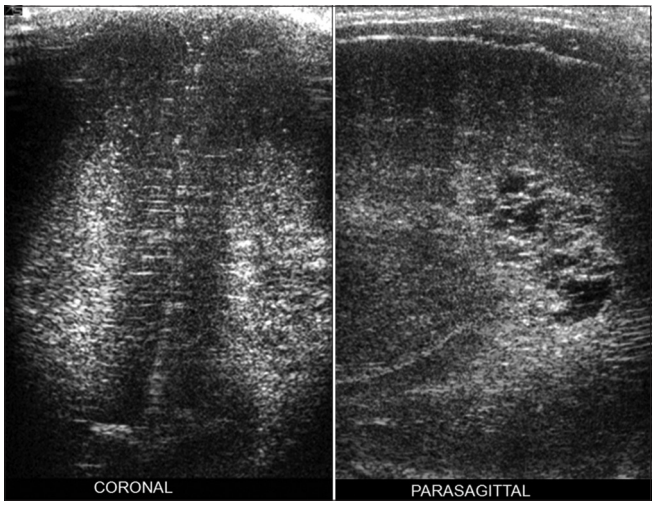

Figure 22A: Coronal USG in a patient demonstrating hyperechoic periventricular parenchyma, sagittal image showing few early cystic changes (grade 2 changes)

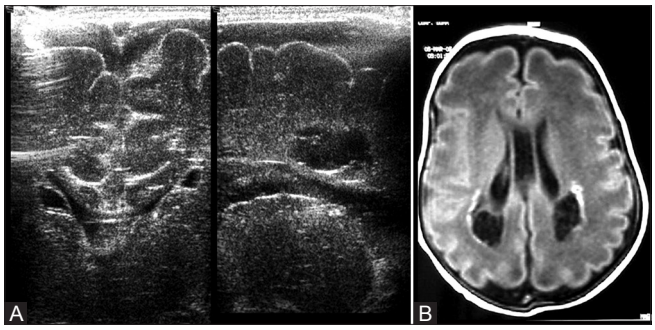

Figure 23 (A, B): Coronal and parasagittal USG demonstrating focal cystic changes in the posterior frontal and the parieto-occipital periventricular region (A). Corresponding axial T1W image (B) demonstrating typical periventricular cystic changes in the peritrigonal region

in assessing the mass effect. The usual observation in the cases of ischemia is a combination of diffuse increase in the echogenicity of ganglionic areas with associated obliteration of cisterns and small capacity of the ventricles [Figure 24].

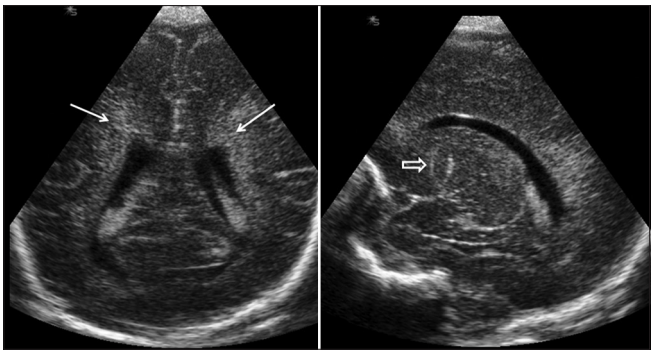

Figure 21: Coronal and parasagittal USG demonstrating a hyperechoic periventricular parenchyma (arrows)(grade 1 changes). There are also changes of mineralizing vasculopathy (open arrow)

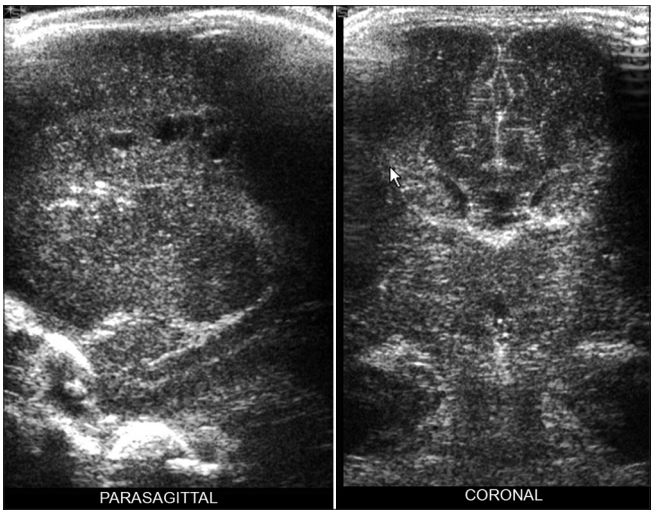

Figure 22B: Cystic PVL changes in posterior frontal region shown by sagittal and coronal USG

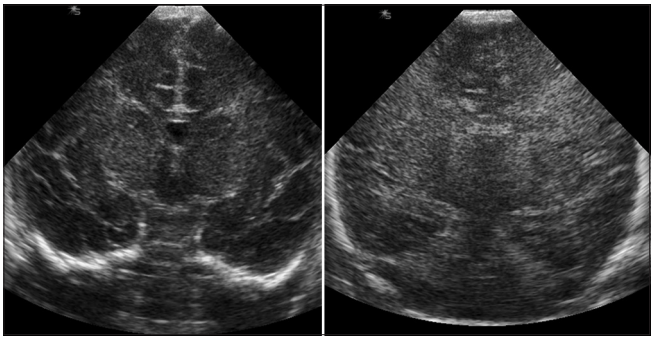

Figure 24: Coronal USG at two levels demonstrating the subtle increase in the cerebral parenchymal echoes in a patient with acute ischemia (secondary to meconium aspiration). Note the small-capacity ventricles and obliterated cisternal spaces

CT and/or magnetic resonance imaging (MRI) still remain as superior techniques in assessing diffuse intracranial ischemia [Figure 25].[17] Serial Doppler examination of the intracranial vessels and circle of Willis is helpful in evaluating the severity of intracranial ischemia. Diastolic flow, reflected in Resistive Index (RI) is a measure that will indicate the hemodynamic status of intracranial flow.[2,12]

Porencephalic Cyst

Large foci of intraventricular/intraparenchymal bleed could lead to a cavitating destructive lesion in the brain parenchyma. After resolution and evacuation of the hematoma, the cavity of the lesion communicates with the ventricular system, leading to the formation of a porencephalic cyst [Figure 26]. Porencephalic cysts, which are, often, a sequel of grade 4 haemorrhages are usually associated with higher neurodevelopmental defects[11]

Congenital CNS Anomalies

Structural information is easily available in premature and mature infants on sonography. Initial evaluation of anomalies can be concluded with reasonable certainty. Hydrocephalus contributes to a large number of cases that can be diagnosed and followed up by neurosonography. Extent of hydrocephalus, level of obstruction, and thickness of the cerebral mantle can be obtained for subsequent follow-up. Biventricular, bifrontal ratio is measured at the level of foramen of Monro for quantitative follow-up of hydrocephalus [Figures 27 and 28]. Grossly dilated ventricular cavities are noted in aqueductal stenosis [Figure 29], agenesis of corpus callosum with midline cyst [Figure 30A and B] and hydrancephaly [Figure 31]. Evaluation through the mastoid fontanelle may be helpful for demonstrating the aqueduct obstruction [Figure 32]. Distinguishing between obstructive versus non-obstructive hydrocephalus is vital, with the former needing neurosurgical consultation for prompt management. Although periventricular transparenchymal passage fluid is not reliably detected in acute obstructions, serial follow-up of ventricular size by sonography helps in distinguishing obstructive, progressive hydrocephalus versus balanced, stable hydrocephalus.

Other anomalies that can be diagnosed using neurosonography include Dandy–Walker syndrome [Figure 33], agenesis of the corpus callosum [Figures 34 and 35], Arnold–Chiari malformation, and vascular malformations. Unusual course of the anterior cerebral artery in cases of agenesis of the corpus callosum, described as sunburst appearance, can be conclusively shown by gray-scale and Doppler examination. Also,

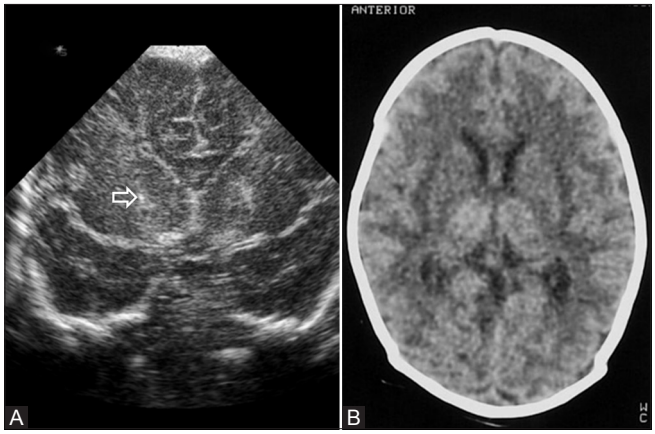

Figure 25 (A, B): Acute ischemic changes demonstrated by coronal USG as the focal hyperechoic (open arrow) changes in the ganglionic areas (A). Corresponding axial non-contrast CT (B) showing the relative decrease in the density of ganglionic areas, a sign of acute ischemia

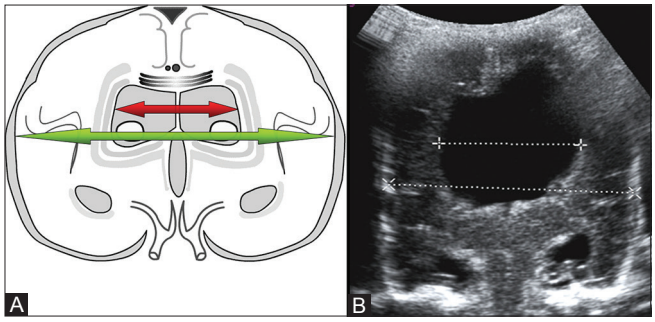

Figure 27 (A, B): Coronal illustration at the level of interventricular foramen, showing the measurements for bifrontal/ventricular ratio (A). USG in a patient with hydrocephalus showing measurement of ventricular/bifrontal ratio (B)

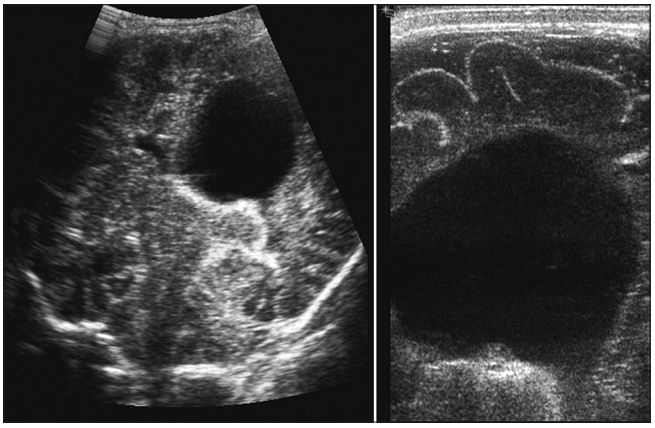

Figure 26: Coronal USG and the high-resolution parasagittal view demonstrating a large porencephalic cyst communicating with the left lateral ventricular cavity. The patient earlier had a large grade 4 hemorrhage

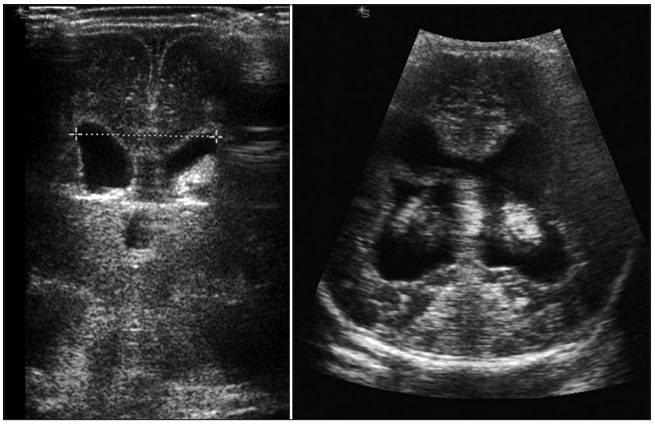

Figure 28: Coronal images at two levels showing hydrocephalus secondary to germinal matrix hemorrhage on the left side. Note the dilated third ventricle due to obstruction at the level of the aqueduct

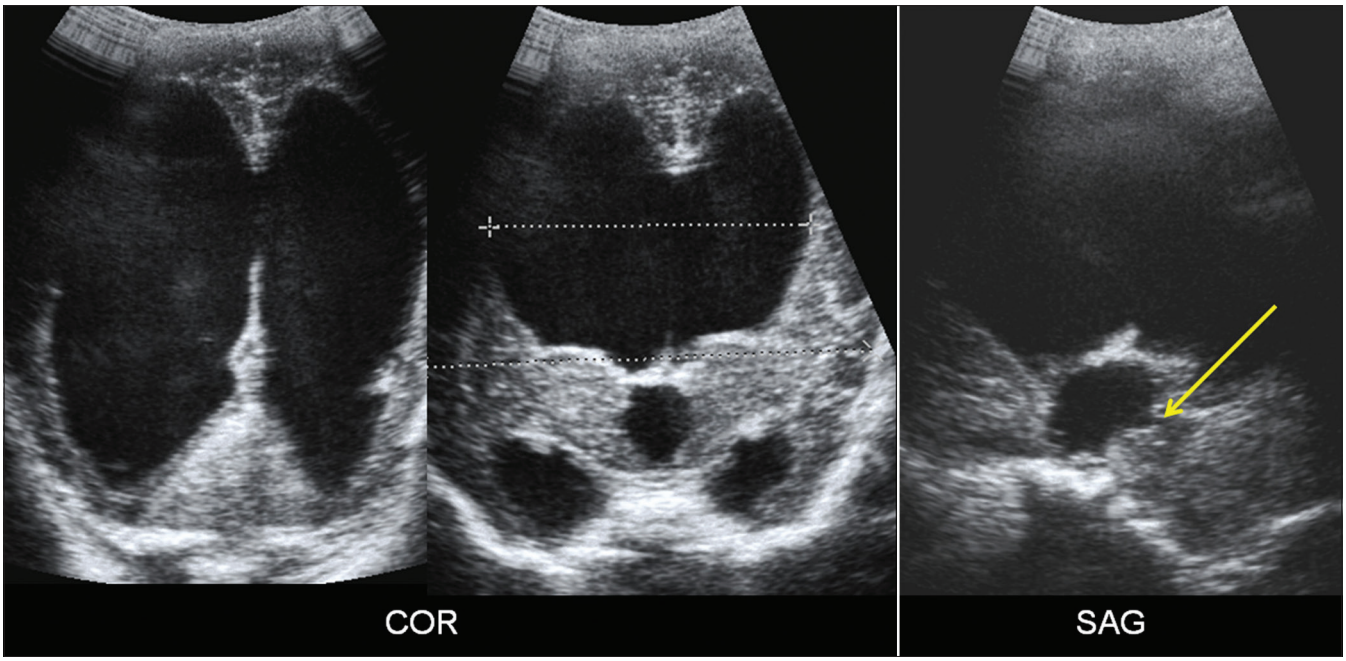

Figure 29: Severe hydrocephalus due to congenital aqueductal stenosis. Sagittal image (C) showing a dilated third ventricle and completely collapsed fourth ventricle. Obstruction is at the level of aqueduct (arrow)

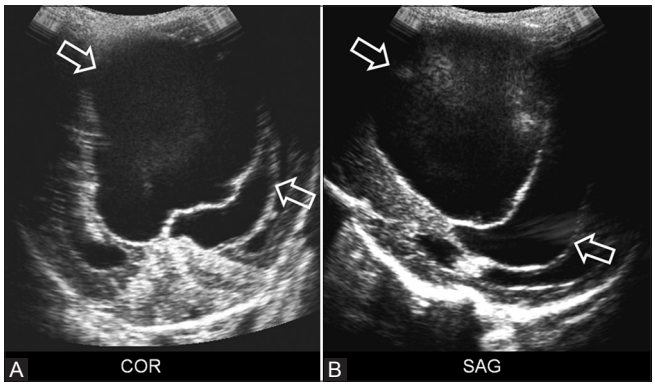

Figure 30 (A, B): (A, B) Coronal and sagittal USG demonstrating severe hydrocephalus in a patient with agenesis of the corpus callosum and midline interhemispheric cyst (open arrows)

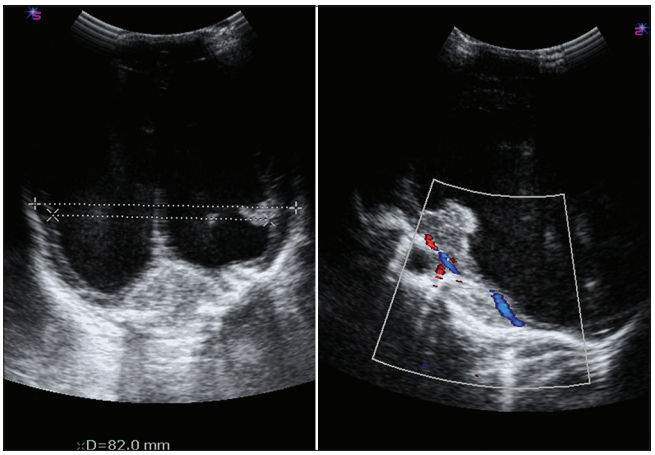

Figure 31: Severe hydrocephalus mimicking hydrancephaly. There is a minimal residual cerebral mantle. Note the small posterior fossa

associated findings like colpocephaly and the additional anomalies of the posterior fossa can be shown [Figure 35]. Hydrancephaly and severe hydrocephalus, although easily demonstrated, cannot be distinguished with certainty on sonography alone. Dysplastic atrophic brain is occasionally seen on sonography. These lesions are seen without the context of ischemia in the early perinatal period. Typically, the brain is small in size, hyperechoic without differentiation of the gray and white matter, and shows multiple cysts of varying size. Lesions are bilateral and often asymmetric [Figure 36A and B]. Direct examination over the cranial swelling can be performed by sonography. Large cephaloceles [Figure 37], dermoid cyst, and cephalhematoma can be diagnosed.

Examination through the mastoid fontanelle can be very useful in differentiating holoprosencephaly from gross hydrocephalus.[7] Additional detailed information regarding the posterior fossa can also be obtained through this route.

Mineralizing Vasculopathy

An appearance of linear bright branching streaks or patches, either unilaterally or bilaterally along the basal ganglia region is suggestive of mineralizing vasculopathy [Figures 38 and 39]. These hyperechoic streaks resembling a branched candlestick are due to the calcification of the walls of the thalamostriatal and lenticulostriatal medium-sized perforating arteries, associated with wall hypercellularity, intramural and perivascular deposition of amorphous basophilic material. Mineralizing vasculopathy is a

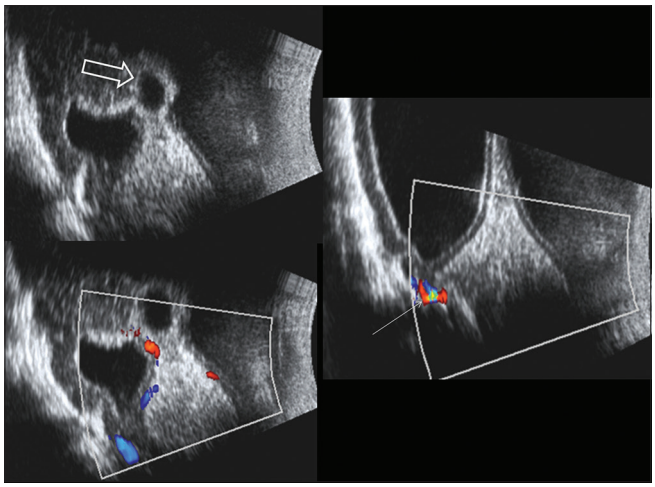

Figure 32: Axial examinations through the mastoid fontanelle showing a total obstruction at the level of the aqueduct. Dilated third ventricle is demonstrated by an open arrow. Incidentally Doppler flow is demonstrated in lateral sinus (long arrow)

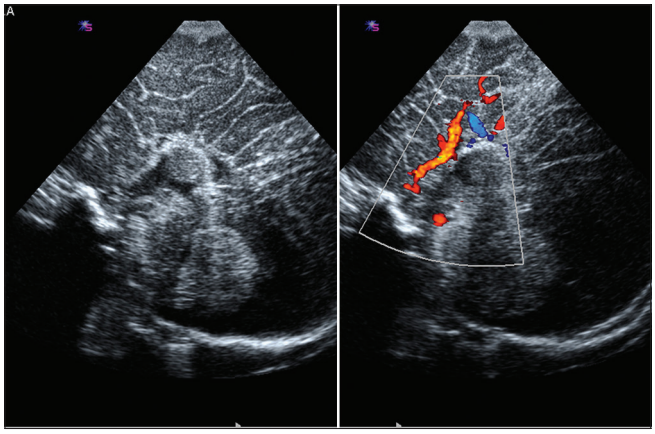

Figure 34: Midline sagittal gray-scale and Doppler images demonstrating agenesis of corpus callosum. Anterior cerebral artery demonstrates vertical course (sunburst appearance). Note the radiating gyri in the frontal area, characteristic of agenesis of the corpus callosum

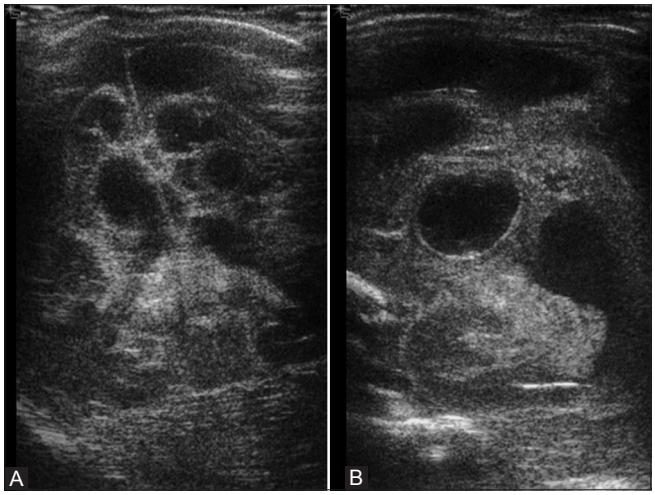

Figure 36 (A, B): (A and B) USG images in two different patients demonstrating dysplastic cerebral parenchyma with hyperechoic and cystic parenchymal changes. Note the gross widening of CSF spaces indicating loss of volume

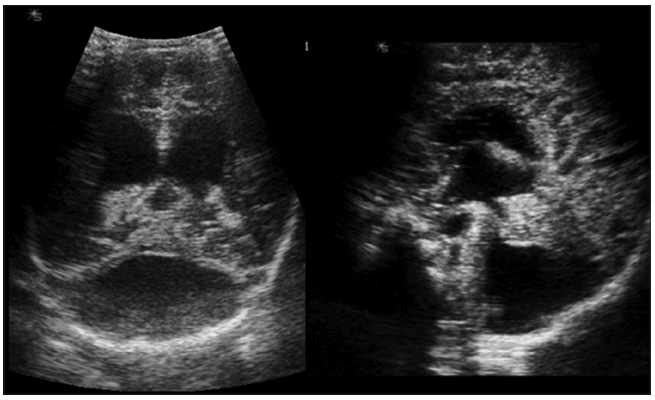

Figure 33: Coronal and sagittal USG demonstrating large posterior fossa cyst in a case of Dandy–Walker syndrome. There is associated moderate hydrocephalus and agenesis of corpus callosum

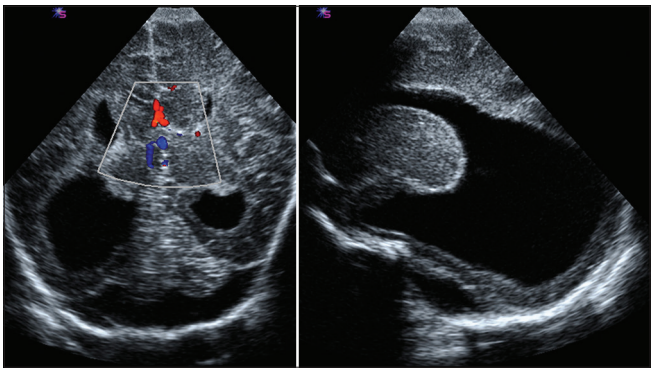

Figure 35: Coronal and parasagittal USG demonstrating colpocephaly in a patient with agenesis of corpus callosum. Also, there is hypoplasia of the cerebellum, mainly involving the right lobe

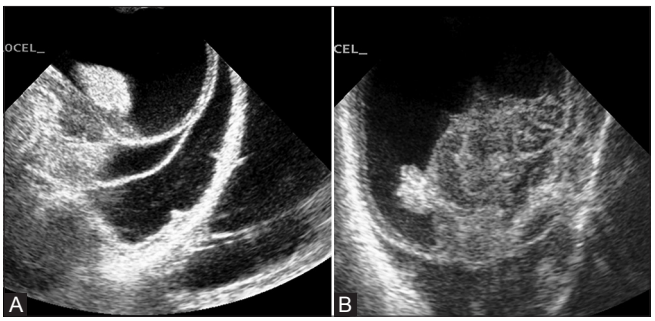

Figure 37 (A, B): Large occipital meningocele with multiple layers of meninges and cystic cerebral parenchyma shown on USG (A). Coronal examination showing the dysplastic cystic changes in the brain (B)

non-specific sign of possible causes ranging from intrauterine TORCH {Toxoplasmosis, Rubella, Cytomegalovirus and Herpes} infections and chromosomal disorders to neonatal asphyxia and maternal drug use.[18]

Vascular Lesions

The dilated vessels of the arteriovenous malformations tend to appear as cystic lesions on neurosonography [Figure 40]. Doppler images might also demonstrate dilated feeding and draining vessels. The typical spectral pattern for

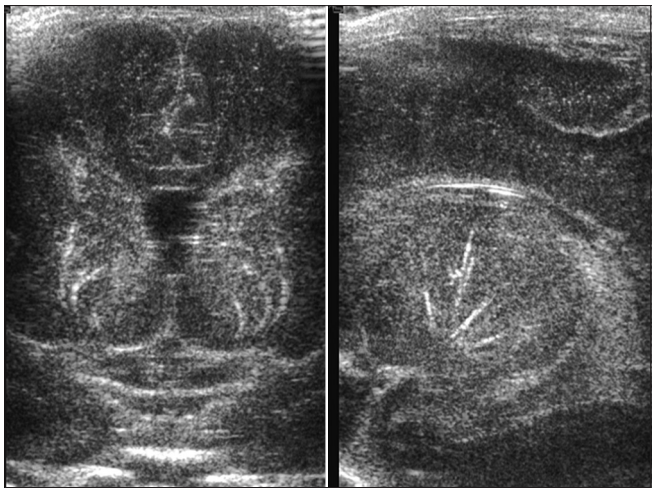

Figure 38: Subtle calcification of the divisions of the middle cerebral artery, demonstrated as hyperechoic linear shadows in bilateral ganglionic regions. Patient also had slightly hyperechoic basal ganglia with small-capacity ventricles due to ischemia. Findings are consistent with the mineralizing vasculopathy

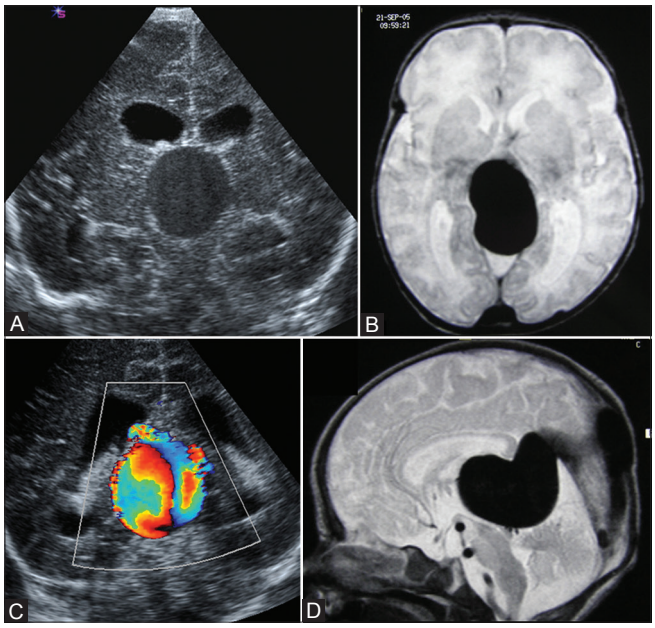

Figure 40 (A-D): Gray-scale and Doppler coronal USG demonstrating a cystic midline structure in the region of posterior third ventricle with mass effect. (A) Typical swirl effect is noted on Doppler (B). Findings are highly suggestive of aneurysmal malformation of the vein of Galen. The corresponding axial and sagittal T2W images of MR examination confirming large aneurysmal dilatation of the vein of Galen (C and D)

intracranial arteriovenous malformations is irregular and biphasic.[19] Small vascular malformations and peripherally located cortical lesions cannot be detected by sonography. However, large asymmetric arteriovenous malformation can be detected by Doppler flow and on demonstration of large feeding veins. Aneurysmal malformation of the vein of Galen is one of the conditions occasionally diagnosed by screening sonography.[19] Typical location of the lesion in posterior-superior third ventricular region between the cerebral hemispheres, with low-level internal echoes and

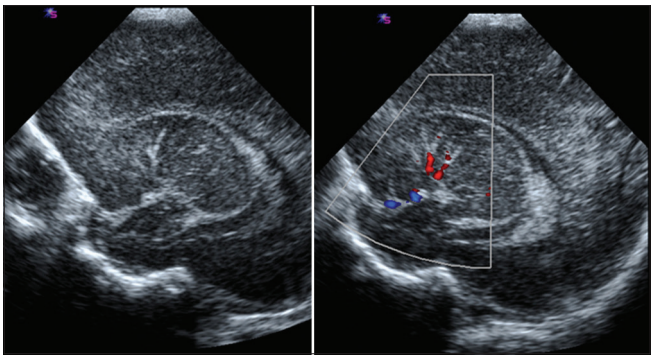

Figure 39: Parasagittal images demonstrating patchy areas of calcification in the branches of middle cerebral artery. Corresponding Doppler image showing patent vessels with wall calcification

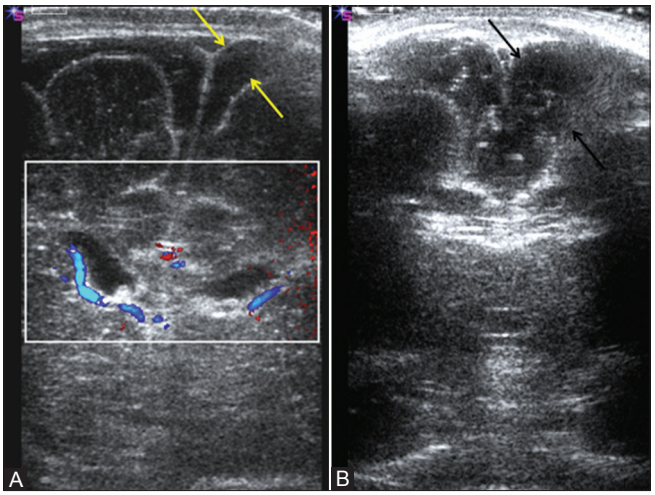

Figure 41 (A, B): (A) High-resolution images of the subarachnoid spaces; normal high-convexity subarachnoid space is demonstrated (yellow arrows). (B) Shows a dilated subarachnoid space with internal echoes in a patient with pyogenic meningitis (black arrows)

swirling effect on Doppler examination makes it possible for a conclusive sonographic diagnosis. Information regarding the feeding arteries and the subtle changes in the parenchyma certainly calls for alternative imaging methods like MRI. Another vascular lesion that can be demonstrated is the thrombosis of the superior sagittal sinus. Although not recommended for routine screening, previously demonstrated thrombus can be followed up by sonographic methods.

Miscellaneous

Intracranial sonography can demonstrate many unsuspected cranial abnormalities. Demonstration of wide subarachnoid spaces with low-level internal echoes is observed in intracranial subarachnoid hemorrhages and meningitis [Figure 41]. The demonstration is facilitated the by use of a high-resolution linear probes. Normal subarachnoid spaces, measured as sinocortical width, are usually less than 3.5 mm wide.[20] Other lesions which can be shown are large mass lesions in the hemispheres,

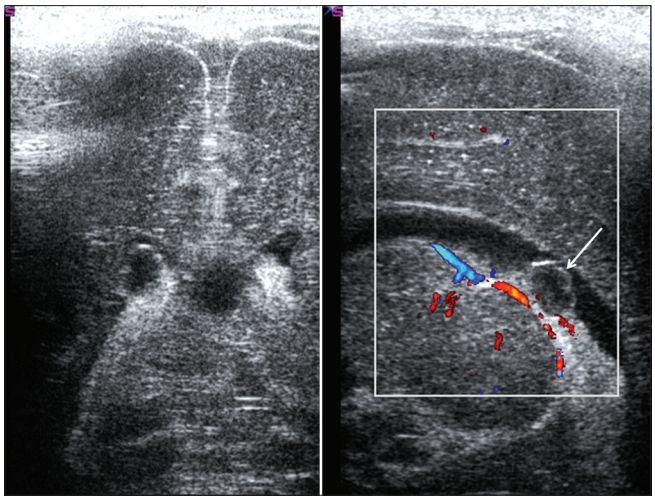

Figure 42: USG images demonstrating incidental observation of a choroid plexus cyst(arrow) in the right lateral ventricle in a syndromic child

notably teratoma, lipoma of corpus callosum, and unusual infantile neuroglial neoplasia arising from cerebral hemispheres. Occasionally, large arachnoid cysts and subdural hematomas are demonstrated by screening examination. Choroid plexus cysts are yet another commonly observed lesion in perinatal sonography. They are incidentally detected in neonates (8.8%), resolving spontaneously without complications when detected in isolation.[21] They may have syndromic associations or may occasionally present as isolated lesions [Figure 42].

Acknowledgment

The authors profoundly thank their neonatology colleagues for their immense support and feedback which made this work a possibility.

References

1. Barkovich AJ. The Encephalopathic Neonate: Choosing the Proper Imaging Technique., AJNR Am J Neuroradiol 1997;18:1816-20.
2. Lowe LH, Bailey Z. State-of-the-Art Cranial Sonography: Part 1, Modern Techniques and Image Interpretation. AJR Am J Roentgenol 2011;196:1028-33.
3. Epelman M, Daneman A, Kellenberger CJ, Aziz A, Konen O, Moineddin R, *et al*. Neonatal encephalopathy: A prospective comparison of head US and MRI. Pediatr Radiol 2010;40:1640-50.
4. Seigel M. Pediatric sonography. 3rd ed. Philadelphia, PA: Lippincott Williams and Wilkins; 2002.
5. Rumack C, Wilson J. Diagnostic ultrasound. Vol 2, Chapter 51. 3rd ed. St. Louis, MO: Mosby; 2005. p. 1624-5.
6. North K, Lowe L. Modern head ultrasound: Normal anatomy, variants, and pitfalls that may simulate disease. Ultrasound Clin 2009;4:497-512.
7. Di Salvo DN. A new view of the neonatal brain: Clinical utility of supplemental neurologic US imaging windows. Radiographics 2001;21:943-55
8. Slovis TL, Kuhns LR. Real-time sonography of the brain through the anterior fontanelle. AJR Am J Roentgenol 1981;136:277-86.
9. Grant EG, Schellinger D, Borts FT, McCullough DC, Friedman GR, Sivasubramanian KN, *et al*. Real- time sonography of the neonatal and infant head. AJR Am J Roentgenol 1981;136:265-70.
10. Farruggia S, Babcock DS. The cavum septi pellucidi: Its appearance and incidence with cranial ultrasonography in infancy. Radiology 1981;139:147-50.
11. Ment LR, Bada HS, Barnes P, Grant PE, Hirtz D, Papile LA, *et al*. Practice parameter: Neuroimaging of the neonate: Report of the Quality Standards Subcommittee of the American Academy of Neurology and the Practice Committee of the Child Neurology Society. Neurology 2002;58:1726-38.
12. Mack LA, Wright K, Hirsch JH, Alvord EC, Guthrie RD, Shuman WP, *et al*. Intracranial hemorrhage in premature infants: Accuracy in sonographic evaluation. AJR Am J Roentgenol 1981;137:245-50.
13. Pape KE, Bennett-Britton S, Szymonowicz W, Martin DJ, Fitz CR, Becker LE. Diagnostic accuracy of neonatal brain imaging: A postmortem correlation of computed tomography and ultrasound scans. J Pediatr 1983;102:275-80.
14. Papile LS, Burstein J, Burstein R, Koffler H. Incidence and evolution of the subependymal intraventricular hemorrhage: A study of infants with weights less than 1500 grams. J Pediatr 1978;92:529-34.
15. Dammann O, Leviton A. Duration of transient hyperechoic images of white matter in very low birth weight infants: A proposed classification. Dev Med Child Neurol 1997;39:2-5.
16. De Vries LS, Eken P, Dubowitz LM. The spectrum of leukomalacia using cranial ultrasound. Behav Brain Res 1992;49:1-6.
17. Sie LT, van der Knaap MS, van Wezel-Meijler G, Taets van Amerongen AH, Lafeber HN, Valk J. Early MR Features of Hypoxic-ischemic Brain Injury in Neonates with Periventricular Densities on Sonograms. AJNR Am J Neuroradiol 2000;21:852-61.
18. Wang HS, Kuo MF, Chang TC. Sonographic lenticulostriate vasculopathy in infants: Some associations and a hypothesis. AJNR Am J Neuroradiol 1995;16:97-102.
19. Cohen HL, Haller JO. Advances in Perinatal Neurosonography. AJR Am J Roentgenol 1994;163:801-10.
20. Armstrong DL, Bagnall C, Harding JE, Teele RL. Measurement of the subarachnoid space by ultrasound in preterm infants. Arch Dis Child Fetal Neonatal Ed 2002;86:F124-6.
21. Hung KL, Liao HT. Neonatal choroid plexus cysts and early childhood developmental outcome. J Formos Med Assoc 2002;101:43-7.

Cite this article as: Bhat V, Bhat V. Neonatal neurosonography: A pictorial essay. Indian J Radiol Imaging 2014;24:389-400.
Source of Support: Nil, **Conflict of Interest:** None declared.